Postdetection optimal diversity combiner for DPSK differential detection

doi: 10.1109/25.231885

Postdetection Optimal Diversity Combiner for DPSK Differential Detection

Fumiyuki Adachi, *Senior Member, IEEE*

Abstract—**Postdetection diversity reception weights and combines all the detector outputs before symbol decision to combat the effects of multipath fading. This paper presents a theoretical analysis of a postdetection optimal diversity combiner that can minimize the symbol error probability for differential phase shift keying (DPSK) differential detection in the presence of multiplicative Rayleigh fading, and co-channel interference (CCI). The effect of unequal average powers among diversity branches is taken into account. It is shown that the postdetection maximal-ratio combiner (MRC) described in [11] and [12] is not optimal unless all branches have the same average power. It is also found that the combiner optimized for the effect of CCI (fading induced random FM noise) should weight each branch detector output in inverse proportion to the average CCI power (desired signal power). Assuming two-branch diversity, calculated BER performance of $\pi/4$-shift QDPSK due to AWGN, CCI, and random FM is presented. In addition, the BER due to multipath channel delay spread (which is not treated in the theoretical analysis) is also computed to find the optimal combiner.**

I. Introduction

DIFFERENTIAL phase shift keying (DPSK) is now attracting much attention for digital cellular mobile radio applications because the required radio channel bandwidth can be much narrower than is possible with constant envelope digital FM [1]–[4]. Digital cellular systems currently under development in both Japan and North America adopt $\pi/4$-shift quartenary DPSK (QDPSK) with Nyquist filtering [5], [6]. Mobile radio channels are characterized by fading caused by interference among multipath waves with different time delays. Fading severely degrades the bit error rate (BER) performance; errors are produced by additive white Gaussian noise (AWGN), random FM noise, and also intersymbol interference (ISI) due to multipath channel delay spread. In cellular mobile radio, the same radio channels should be reused in spatially separated cells as close to each other as possible to use the limited frequency spectrum efficiently; co-channel interference (CCI) becomes another important cause of error. Diversity reception is one of the most powerful techniques to combat the fading effects.

Basically, there are two types of diversity combiners: the predetection type and the postdetection type. A predetection diversity combiner cophases, weights, and combines all signals received on the different branches before signal detection. Well-known predetection combiners are the selection combiner (SC), equal-gain combiner (EGC), and the maximal-ratio combiner (MRC) [7, ch. 10, 11], [8, ch. 6], [9]. Recently, an MMSE diversity combiner specifically designed to combat ISI due to delay spread was proposed [10]. These predetection diversity combiners require several complicated functions, such as a function to cophase all received signals which suffer fading induced fast random phase variations. On the other hand, postdetection diversity combiners weight and combine all branches after signal detection and do not require the difficult-to-implement cophasing function. Since the combiner structure can be much simpler, postdetection diversity is more practically attractive for mobile radio. A postdetection MRC[1] was proposed and investigated for digital FM and DPSK with differential detection [8, ch. 6.7], [11], [12]. It yields larger diversity gain than postdetection SC; it was found [11], [12] that a 1.5-dB larger diversity gain can be achieved with a two-branch combiner.

In previous analyses of postdetection diversity [8], [11], [12], all branches were assumed to suffer from independent Rayleigh fading with the same average power. However, this assumption is seldom true in practical situations[2]. Recently, Adachi *et al.* investigated the BER performance of $\pi/4$-shift QDPSK with a two-branch postdetection SC and showed that unequal power degrades the performance [13]. In these nonideal situations, however, the BER performance can be improved if each branch differential detector output is weighted, before combination, according to its channel condition. In this paper, we theoretically analyze the postdetection optimal diversity combiner for DPSK differential detection in the presence of fading and CCI. The analysis assumes that the received signal on each branch suffers from independent, multiplicative Rayleigh fading with unequal average power. Section II describes the transmission model. Section III examines the maximum-likelihood symbol-by-symbol decision to find the optimal combiner. It will be shown that postdetection MRC is optimal only when all branches have the same average power. Section IV numerically evaluates the BER performance of $\pi/4$-shift QDPSK with two-branch optimal diversity. This section also investigates the optimal combiner

Manuscript received March 19, 1992; revised May 21, 1992.

The author is with NTT Mobile Communications Network, Inc., Yokosuka-shi, Kanagawa-Ken, Japan.

IEEE Log Number 9207172.

[1] The term MRC is used here for convenience because it is analogous to the well-known predetection MRC (see Section V). Each branch differential detector output is weighted, before combination, in proportion to the squared value of the detector input envelope when a hard-limiter is used at the detector input. This is mathematically equivalent to the combination of all detector outputs with equal weight when no hard-limiter is applied.

[2] Unequal average powers are produced by differences in the gain of each diversity antenna. In particular, for hand-held portable transceivers, the built-in diversity antenna scheme produces an antenna gain difference of about 1 dB [14].

for frequency-selective Rayleigh fading (which is not treated in the theoretical analysis).

II. Transmission Model

A mathematical block diagram for M-ary DPSK transmission with L-branch postdetection diversity reception is shown in Fig. 1. π/M-shift (or symmetrical) Gray mapping is considered; a $\log 2M$-bit symbol is mapped to the differential phase $\Delta\phi(k) = \phi(k) - \phi(k-1)$, where $\phi(k)$ is the kth phase of the carrier, and $\Delta\phi(k) = (2m + 1 - M)\pi/M$ with $m = 0, 1, 2, \cdots, M-1$. The transmitted signal is

$$s(t) = \sum_{k=-\infty}^{+\infty} h_T(t - kT) \cdot \exp j\phi(k) \tag{1}$$

where $h_T(t)$ is the impulse response of the transmitter filter and T is the symbol duration. The signal is transmitter over a multipath channel and received at L different antennas. The AWGN and faded CCI are added to the desired signal, and they are passed through the receiver filter having impulse response $h_R(t)$ to be differentially detected. No hard-limiter is assumed at the detector input. The lth $(l = 1, 2, \cdots, L)$ branch detector input can be represented in the complex form as

$$z_l(t) = \sqrt{\frac{2E_{sl}}{T}} \int_{-\infty}^{+\infty} d_s(t-\tau) g_l(\tau, t) d\tau + z_{il}(t) + z_{nl}(t) \tag{2}$$

where $d_s(t)$ is the overall filter (the transmitter and receiver filters) response to (1), E_{sl} is the average received signal energy per symbol, $z_{il}(t)$ is the CCI complex envelope, and $z_{nl}(t)$ is the filtered AWGN with a power of N_0/T (N_0 is the single-sided AWGN power spectrum density). Assuming squareroot raised cosine Nyquist filters with roll-off factor α at the transmitter and receiver, $d_s(t)$ is given by

$$\begin{aligned} d_s(t) &= s(t) \otimes h_R(t) \\ &= \sum_{k=-\infty}^{+\infty} \exp j\phi(k) \frac{\sin(\pi(t-kT)/T)}{\pi(t-kT)/T} \\ &\quad \cdot \frac{\cos(\alpha\pi(t-kT)/T)}{1 - (2\alpha(t-kT)/T)^2} \end{aligned} \tag{3}$$

where $\otimes$ denotes convolution. In (2), $g_l(\tau, t)$ is the multipath channel complex impulse response, measured from the instant of application of a unit impulse at the transmitter at time t. In urban areas, many impulses are produced by reflections from numerous obstacles surrounding the mobile; $g_l(\tau, t)$ results in a zero-mean complex Gaussian process of time t according to the central limit theorem. This model was also adopted in [9]–[12]. Frequency selectivity of the channel can be determined by the rms delay spread (defined in Section IV-C). If the rms delay spread is very small compared to the symbol duration, many impulses arrive at almost the same time at the receiver antenna. In this case, the delay spread effect can be neglected, and $g_l(\tau, t)$ can be approximated as $g_l(\tau, t) = g_l(t)\delta(\tau)$, resulting in multiplicative Rayleigh fading. Section III assumes this multiplicative Rayleigh fading.

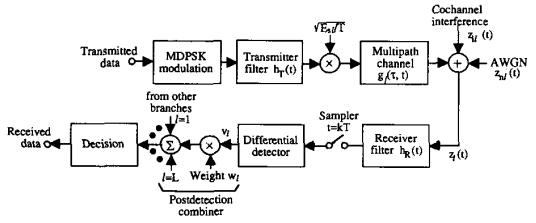

Fig. 1. Transmission model.

The frequency selective Rayleigh fading case will be treated in Section IV-C.

The differential detector input $z_l(t)$ is sampled at $t = kT$ (we assume ideal sampling timing) and is denoted by $z_l(k)$. We assume the conventional one-symbol differential detector which multiplies $z_l(k)$ with $k_l^*(k-1)$ to produce the output

$$v_l = z_l(k) \cdot z_l^*(k-1) \tag{4}$$

where * denotes the complex conjugate. The postdetection combiner considered here produces the sum of weighted samples of L differential detector outputs. The symbol decision is performed based on the combiner output

$$v = \sum_{l=1}^{L} w_l \cdot v_l \tag{5}$$

where w_l is the lth branch weight. In this paper, we will find the optimal weight that minimizes the symbol error probability.

III. Optimal Combiner

First, we derive an optimal combiner for no fading by examining the maximum-likelihood symbol-by-symbol decision, and then we extend our analysis to the multiplicative Rayleigh fading case.

A. No Fading

Fading and CCI are assumed to be absent. The channel is time invariant, and thus $g_l(\tau, t) = \delta(\tau) \exp j\theta_l$ where θ_l is the arbitrary random phase. Moreover $d_s(k) = \exp j\phi(k)$ because of ideal sampling timing. Equation (2) can be rewritten as

$$z_l(k) = \sqrt{\frac{2E_{sl}}{T}} \exp j[\phi(k) + \theta_l] + z_{nl}(k) \tag{6}$$

which is a complex Gaussian variable with mean $\sqrt{2E_{sl}/T} \exp j[\phi(k) + \theta_l]$ and variance N_0/T. In differential detection, $z_l(k-1)$ is the reference signal. For the given kth symbol and $z_l(k-1)$ (note that θ_l is also given), it is apparent that $v_l = z_l(k)z_l^*(k-1)$ becomes a complex Gaussian variable with mean $\sqrt{2E_{sl}/T} \exp j[\phi(k) + \theta_l] \cdot z_l^*(k-1)$ and variance $(N_0/T)\,|z_l(k-1)|^2$. Since $\exp j[\phi(k) + \theta_l] = \exp j\Delta\phi(k) \cdot \exp j[\phi(k-1) + \theta_l]$, the probability density function (pdf) of the conditional detector output v_l can be expressed from [7, appendix B] as (7), shown at the bottom of the next page.

Assuming that all symbols are equally likely, the kth symbol decision can be based on computing the likelihood function $Q_m = \prod_{l=1}^{L} p(v_l | z_l(k-1), \Delta\phi(k) = \Delta\phi_m)$, where

$m = 0, 1, 2, \cdots, M-1$, and the receiver decides that $\Delta\phi_j$ was transmitted if $Q_j = \max Q_m$. Taking the logarithm of Q_m, the log-likelihood function can be expressed as

$$\log Q_m = \mathrm{Re}\left[\sum_{l=1}^{L} v_l \exp[-j\Delta\phi_m] \cdot \frac{z_l(k-1)\left(\sqrt{\frac{2E_{sl}}{T}}\exp j[\phi(k-1)+\theta_l]\right)^*}{(N_0/T)\,|z_l(k-1)|^2}\right] + \text{constant} \tag{8}$$

where $\mathrm{Re}[z]$ denotes the real part of the complex value z. The terms which do not affect the likelihood decision are represented as "constant." The process implied by (8) cannot be realized, since the signal component $\sqrt{2E_{sl}/T}\exp j[\phi(k-1)+\theta_l]$ is unknown (only v_l's are available). To find an implementable solution, we replace $\sqrt{2E_{sl}/T}\exp j[\phi(k-1)+\theta_l]$ by its best estimate (in the maximum likelihood sense) which is $z_l(k-1)$ (see Appendix A). Now we obtain $\log Q_m = \mathrm{Re}\left[\sum_{l=1}^{L} v_l \cdot \exp -j\Delta\phi_m\right] \;/\; (N_0/T) +$ constant. Neglecting the common constant and coefficient, the decision problem can be reduced to finding m that maximizes

$$\lambda_m = \mathrm{Re}[v \cdot \exp -j\Delta\phi_m] \tag{9}$$

where

$$v = \sum_{l=1}^{L} v_l\,. \tag{10}$$

Compare (5) and (10). All branch detector output samples are simply summed with $w_l = 1$, as in the postdetection MRC described in [11] and [12]. This is identical to Voelcker's result for BDPSK ($M = 2$) [15].

B. Multiplicative Rayleigh Fading

We consider that both the desired signal and CCI suffer from multiplicative Rayleigh fading. We assume independent fading for all L branches. Since $g_l(\tau, t) = g_l(t)\delta(\tau)$, the lth branch detector input sampled at $t = kT$ can be expressed as

$$z_l(k) = \sqrt{\frac{2E_{sl}}{T}}\, g_l(k)\exp j\phi(k) + z_{il}(k) + z_{nl}(k) \tag{11}$$

where $g_l(k)$ is a zero-mean complex Gaussian variable with $\langle |g_l(k)|^2 \rangle = 1$. We assume a single CCI that is also DPSK-modulated with identical timing to the desired signal. The faded CCI sample $z_{il}(k)$ can be expressed in a similar form to the desired signal, and both $z_{il}(k)$ and $z_{il}(k-1)$ are zero-mean complex Gaussian variables. However, their cross-correlation is affected by the CCI transmitted symbol. Most decision errors are produced when the instantaneous amplitude of the CCI surpasses that of the desired signal. Since the amplitude variation is significantly determined by Rayleigh fading itself, the effect of modulation is less important. Therefore, we use an approximation that two consecutive CCI samples are statistically independent. (If we assume multiple CCI with different transmitted symbol sequences, cross-correlation between $z_{il}(k)$ and $z_{il}(k-1)$ approaches zero. In this case, the assumption that two consecutive samples are independent is valid.)

The detector output samples, $z_l(k)$ and $z_l(k-1)$, are mutually correlated complex Gaussian variables. It can be shown from [11] that for the given kth symbol and $z_l(k-1)$, $z_l(k)$ becomes a complex Gaussian variable with mean $z_l(k-1)\rho_l(\sigma_l/\sigma_l')$ and variance $\sigma_l^2(1-|\rho_l|^2)$, where $\sigma_l^2 = 1/2\langle |z_l(k)|^2 \rangle$, $\sigma_l'^2 = 1/2\langle |z_l(k-1)|^2 \rangle$, and $\rho_l = 1/2\langle z_l(k) z_l^*(k-1)\rangle/(\sigma_l\sigma_l')$. The conditional pdf of differential detector output v_l can be given by

$$p(v_l|z_l(k-1), \Delta\phi(k)) = \frac{1}{2\pi\sigma_l^2\left(1-|\rho_l|^2\right)|z_l(k-1)|^2} \cdot \exp\left[-\frac{\left|v_l - \rho_l\frac{\sigma_l}{\sigma_l'}|z_l(k-1)|^2\right|^2}{2\sigma_l^2\left(1-|\rho_l|^2\right)|z_l(k-1)|^2}\right] \tag{12}$$

where σ_l, σ_l', and ρ_l are given by

$$\sigma_l^2 = \sigma_l'^2 = \frac{E_{sl}}{T} + \frac{E_{il}}{T} + \frac{N_0}{T} = \frac{N_0}{T}\,\Gamma_l\left(1 + \Gamma_l^{-1} + \Lambda_l^{-1}\right)$$
$$\rho_l = \eta\,\frac{\exp j\Delta\phi(k)}{1 + \Gamma_l^{-1} + \Lambda_l^{-1}}\,. \tag{13}$$

E_{sl} and E_{il} are the average desired signal energy and the average CCI energy per symbol, respectively, $\Gamma_l = E_{sl}/N_0$ is the average signal energy per symbol-to-noise power spectrum density ratio (E_s/N_0), $\Lambda_l = E_{sl}/E_{il}$ is the average signal-to-interference power ratio (SIR), and $\eta = \langle g_l(k) g_l^*(k-1)\rangle$ is the fading correlation, which is assumed to be the same for all branches.

ρ_l is a function of the differential phase $\Delta\phi(k)$ corresponding to kth transmitted symbol; hereafter, we use the new notation $\rho_l(\Delta\phi(k))$ to indicate explicitly that it involves $\Delta\phi(k)$. Since σ_l, σ_l' and $|\rho_l(\Delta\phi(k))|$ do not involve the

$$p(v_l|z_l(k-1), \Delta\phi(k)) = \frac{1}{2\pi(N_0/T)\,|z_l(k-1)|^2}\exp\left[-\frac{\left|v_l - \exp j\Delta\phi(k) z_l^*(k-1)\left(\sqrt{\frac{2E_{sl}}{T}}\exp j[\phi(k-1)+\theta_l]\right)\right|^2}{2(N_0/T)\,|z_l(k-1)|^2}\right]. \tag{7}$$

modulation term, the optimal decision can be based on computing the following log-likelihood function:

$$\log Q_m = \log \prod_{l=1}^{L} p(v_l | z_l(k-1), \Delta\phi(k) = \Delta\phi_m)$$
$$= \mathrm{Re}\left[\sum_{l=1}^{L} \frac{v_l}{\sigma_l \sigma_l'} \frac{\rho_l^*(\Delta\phi_m)}{1 - |\rho_l(\Delta\phi_m)|^2}\right] + \text{constant}. \quad (14)$$

The terms that do not involve $\Delta\phi_m$, and hence do not affect the likelihood decision, are represented as "constant." Substituting (13) into (14), we have

$$\log Q_m = \mathrm{Re}\left[\left(\frac{\eta^*}{N_0/T} \sum_{l=1}^{L} \cdot \frac{\Gamma_l^{-1}}{\left(2 + \Gamma_l^{-1} + \Lambda_l^{-1}\right)\left(\Gamma_l^{-1} + \Lambda_l^{-1}\right) + 1 - |\eta|^2} v_l\right) \cdot \exp -j\Delta\phi_m\right] + \text{constant}. \quad (15)$$

From (15), the decision problem can be reduced to finding m that maximizes

$$\lambda_m = \mathrm{Re}[v \cdot \exp -j\Delta\phi_m] \quad (16)$$

where v is given by

$$v = \sum_{l-1}^{L} w_l \cdot v_l = \sum_{l=1}^{L} \frac{a\Gamma_l^{-1}}{\left(2 + \Gamma_l^{-1} + \Lambda_l^{-1}\right)\left(\Gamma_l^{-1} + \Lambda_l^{-1}\right) + 1 - |\eta|^2} v_l. \quad (17)$$

Equation (17) is the optimal combiner for the Rayleigh fading case. The common coefficient "a" is introduced to obtain simpler expressions later for the optimal weight.

The optimal combiner for no fading simply sums up all the detector outputs with equal weight. This is not optimal any more in the presence of fading. However, when all branches have the same average signal power and the same average CCI power, i.e., $\Gamma_l = \Gamma$ and $\Lambda_i = \Lambda$ for all l, the weight w_l becomes the same for all branches, and the optimal combiner reduces to that for the no fading case (or postdetection MRC). Since we used the approximation that two consecutive CCI samples, $z_{il}(k)$ and $z_{il}(k-1)$, are independent, strictly speaking, the diversity combiner given by (17) is approximately optimal. However, it should be noted that it is optimal when CCI does not exist ($\Lambda_l \to \infty$).

C. Discussions

For the very slow fading case ($\eta \to 1$), from (17) the optimal weight is given by

$$w_l = \frac{a\Gamma_l^{-1}}{\left(2 + \Gamma_l^{-1} + \Lambda_l^{-1}\right)\left(\Gamma_l^{-1} + \Lambda_l^{-1}\right)}. \quad (18)$$

The prediction of the average powers of both the desired signal and CCI is required. In order to see more clearly the role of the weight, we consider the cases of AWGN limited channel and CCI limited channel separately. When $\Lambda_l \to \infty$ for all l, AWGN is the single cause of errors (AWGN limited channel). Letting $a = 2$, (18) becomes

$$w_l = \frac{\Gamma_l}{\Gamma_l + 0.5} \quad (19)$$

which is different from the optimal weight ($w_l = 1$) for no fading case. The optimal weight for no fading was derived by using $z_l(k-1)$ as the best estimate of $\sqrt{2E_{sl}/T}\exp j[\phi(k-1)+\theta_l]$. This estimate becomes unreliable for small E_s/N_0 values. For fading with unequal average powers, the instantaneous E_s/N_0 of the branch with smaller average E_s/N_0 drops more frequently, and thus its contribution to the combiner output should be decreased. Consequently, using equal weights is no longer optimal. However, it can be seen from (19) that when Γ_l is larger than, e.g., 10 dB for all L branches, $w_l \sim 1$, and thus equal weights may be used (this will be discussed in Section IV). On the other hand, when $\Gamma_l \to \infty$ for all l, the CCI becomes the single cause of errors (CCI limited channel). In this case, w_l approaches $w_l = a(\Lambda_l/\Gamma_l)/(2 + \Lambda_l^{-1})$. Since $\Lambda_l = E_{sl}/E_{il}$ and $\Gamma_l = E_{sl}/N_0$, we have $\Lambda_l/\Gamma_l = N_0/E_{il}$. Define the CCI power ratio as $q_{il} = E_{il}/\max E_{il}$ so that the branch with the maximum power has $q_{il} = 1$ (the lth branch average CCI power is normalized by the maximum value among L branches). Letting $a = 2 \max E_{il}/N_0$, (18) becomes

$$w_l = q_{il}^{-1} \frac{\Lambda_l}{\Lambda_l + 0.5}. \quad (20)$$

This implies that the branch weights should be inversely proportional to the average CCI power for large average SIR's.

Fading produces random FM noise (or random phase noise, given by $\Delta\theta_l = \arg[g_l(k)g_l^*(k-1)]$. When both Γ_l and $\Lambda_l \to \infty$, random FM noise becomes the single cause of errors (random FM noise limited channel). From (17), a prediction of the fading correlation is required. However, this may not be possible in practice. In the following, we derive an implementable solution which does not require the prediction of the fading correlation. First, we let $\Lambda_l \to \infty$ (no CCI) in (17) to obtain $w_l = a/\left[2 + \Gamma_l^{-1} + \Gamma_l\left(1 - |\eta|^2\right)\right]$ which approaches $a\Gamma_l^{-1}/\left(1 - |\eta|^2\right)$ as $\Gamma_l \to \infty$. Recall that $\Gamma_l = E_{sl}/N_0$ and define the desired signal power ratio as $q_{sl} = E_{sl}/\max E_{sl}$ so that the branch with the maximum power has $q_{sl} = 1$. Letting $a = \left(1 - |\eta|^2\right)\max E_{sl}/N_0$, w_l can be expressed as

$$w_l = q_{sl}^{-1}. \quad (21)$$

The branch weight should be inversely proportional to the average desired signal power.

It can be seen from (20) and (21) that the contribution to the combiner output from the branch with larger average (desired signal or CCI) power should be made smaller. The reason for this is qualitatively explained below. Consider a CCI limited channel. Since $v_l = z_l(k)z_l^*(k-1)$, the magnitude of v_l is proportional to the average desired signal-plus-CCI power of the lth branch. If the same weight is used for all branches, the contribution of the larger average power branch to the

combiner output becomes larger. The symbol error probability is governed by the average SIR, not by the average desired signal-plus-CCI power. Thus the use of equal weights degrades performance. The optimal weight of (20) can be interpreted as equalizing all branches so as to achieve the same average CCI power; thus the branch with larger average SIR has a larger contribution to the combiner output. A similar discussion can be applied to the random FM noise limited channel.

IV. BER Analysis

Although the postdetection optimal diversity combiner derived in Section III is valid for M-ary DPSK (MDPSK), this paper is most interested in linear $\pi/4$-shift QDPSK. Furthermore, the most practical diversity reception is to use two spatially separated antennas. In Section IV-A, the average BER performance of differentially detected $\pi/4$-shift QDPSK is theoretically analyzed for two-branch postdetection optimal diversity. The numerical results for the multiplicative fading case are presented in Section IV-B. For high bit rate transmission, however, fading becomes frequency selective, and the effect of multipath channel delay spread cannot be neglected. Section IV-C considers the optimal diversity combiner for the frequency selective fading.

A. Analysis of Average BER

For $\pi/4$-shift QDPSK, the set of four differential phases is used: $\Delta\phi_m = (2m-3)\pi/4$, $m = 0, 1, 2$, and 3. Assuming the Gray mapping rule, the two-bit symbol (a_k, b_k) is mapped to the differential phase as

$$\Delta\phi(k) = \begin{cases} 3\pi/4 \\ \pi/4 \\ -\pi/4 \\ -3\pi/4 \end{cases} \quad \text{for } (a_k, b_k) = \begin{cases} (-1,1) \\ (1,1) \\ (1,-1) \\ (-1,-1) \end{cases} . \tag{22}$$

The constellation of the signal space is shown in Fig. 2. For this type of modulation, the polarity of the real (imaginary) part of the differential detector output v_l corresponds to the sign of $a_k(b_k)$ of the transmitted symbol. The maximum-likelihood decision suggested in Section III (see (9) and (16)) is equivalent to performing independent binary decision on a_k and b_k, respectively, based on the polarities of the real and imaginary parts of the combiner output v. Bit errors are then produced when $a_k \cdot \mathrm{Re}[v] < 0$ and when $b_k \cdot \mathrm{Im}[v] < 0$. For the symmetrical power spectra of filtered AWGN and fading complex envelope, the average BER's for a_k and b_k are identical. Therefore, it is sufficient to consider the error probability of a_k only.

It was shown in Section III-B (see (12)) that for the given $z_l(k-1)$, the lth branch detector output v_l becomes a complex Gaussian variable with mean $\rho_l(\sigma_l/\sigma_l')\,|z_l(k-1)|^2$ and variance $\sigma_l^2\left(1-|\rho_l|^2\right)|z_l(k-1)|^2$. (For multiplicative fading, $\sigma_l = \sigma_l'$ from (13). However, for frequency-selective fading, this doesn't hold because of ISI effect, so the term σ_l/σ_l' is left here.) Since optimal combining is a linear combination of the weighted samples of the detector outputs, the combiner output sample v also becomes a complex Gaussian variable

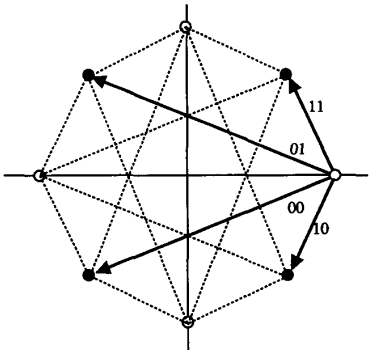

Fig. 2. Constellation of $\pi/4$-shift QDPSK.

with mean m and variance σ^2:

$$m = m_c + jm_s = \sum_{l=1}^{2} w_l \cdot \rho_l \cdot \frac{\sigma_l}{\sigma_l'} |z_l(k-1)|^2$$

$$\sigma^2 = \sum_{l=1}^{2} w_l^2 \sigma_l^2 \left(1 - |\rho_l|^2\right) |z_l(k-1)|^2 . \tag{23}$$

Therefore, for the given a_k, $x = a_k \cdot \mathrm{Re}[v]$ becomes a Gaussian variable with mean $a_k m_c$ and variance $\sigma^2 (= a_k^2 \sigma^2)$. The BER conditioned on $|z_1| = |z_1(k-1)|$ and $|z_2| = |z_2(k-1)|$ can be calculated from

$$p_e(|z_1|, |z_2|) = \int_{-\infty}^{0} \frac{1}{\sqrt{2\pi}\,\sigma} \exp\left[-\frac{(x - a_k m_c)^2}{2\sigma^2}\right] \mathrm{dx}$$

$$= \frac{1}{2} \operatorname{erfc}\left[\frac{a_k m_c}{\sqrt{2}\,\sigma}\right] . \tag{24}$$

To simplify the succeeding derivation, we introduce the following variable transformation: $|z_1| = R\cos\psi$ and $|z_2| = R\sin\psi$, where $0 \leqq R$ and $0 \leqq \psi \leqq \pi/2$. Substituting (23) into (24), we now obtain

$$p_e(R, \psi) = \frac{1}{2} \cdot \operatorname{erfc}\left[\frac{w_1(a_k\rho_{1c})\,(\sigma_1/\sigma_1')\cos^2\psi + w_2(a_k\rho_{2c})\,(\sigma_2/\sigma_2')\sin^2\psi}{\sqrt{w_1^2\sigma_1^2\left(1-|\rho_1|^2\right)\cos^2\psi + w_2^2\sigma_2^2\left(1-|\rho_2|^2\right)\sin^2\psi}} \cdot \frac{R}{\sqrt{2}}\right] \tag{25}$$

where $\rho_l = \rho_{lc} + j\rho_{ls}$. For the mapping rule described in (22), $\exp j\Delta\phi(k) = (a_k + jb_k)/\sqrt{2}$. It can be found from (13) that $\rho_l = \eta\{(a_k + jb_k)/\sqrt{2}\}/\left(1 + \Gamma_l^{-1} + \Lambda_l^{-1}\right)$; therefore $a_k\rho_{lc}$ has a value of $(\eta/\sqrt{2})/\left(1 + \Gamma_l^{-1} + \Lambda_l^{-1}\right)$ and is always positive.

The conditional BER should be averaged over the statistics of R and ψ. The joint pdf $p(R, \psi)$ can be found from that of $|z_1|$ and $|z_2|$ which is given by $p(|z_1|, |z_2|) = p(|z_1|)\cdot p(|z_2|) = |z_1||z_2|/(\sigma_1'^2\sigma_2'^2)\,\exp\left[-|z_1|^2/(2\sigma_1'^2) - |z_2|^2/(2\sigma_2'^2)\right]$ (recall that $\sigma_l'^2 = 1/2\langle|z_l(k-1)|^2\rangle$). The Jacobian of the variable

transformation from $|z_1|$ and $|z_2|$ to R and ψ is R, and we have

$$p(R,\psi) = \frac{R^3 \sin\psi\cos\psi}{\sigma_1'^2\sigma_2'^2} \cdot \exp\left[-\frac{R^2}{2}\left(\frac{\cos^2\psi}{\sigma_1'^2}+\frac{\sin^2\psi}{\sigma_2'^2}\right)\right]. \quad (26)$$

Integration of $p_e(R,\psi)\cdot p(R,\psi)$ with respect to R can be performed, and the average BER calculation reduces to a single integration (see Appendix B):

$$P_e = \int_0^{\frac{\pi}{2}} \alpha\left[1 - \frac{\beta}{\sqrt{1+\beta^2}} - \frac{1}{2}\frac{\beta}{(1+\beta^2)^{3/2}}\right] d\psi. \quad (27)$$

α and β in (27) are defined in (28) at the bottom of the page.

In particular, when the two branches suffer statistically independent, identically distributed multiplicative fading (both branches have the same average desired signal power and the same average CCI power), we have $\sigma_1 = \sigma_2$, $\sigma_1' = \sigma_2'$, and $\rho_1 = \rho_2$. In this case, from Section III-B, the weights w_1 and w_2 should be equal. Since $\alpha = \sin(2\psi)/2$ and β does not involve ψ, integration in (27) can now be performed, and we arrive at a simple result:

$$P_e = \frac{1}{2}\left[1 - \frac{\beta}{\sqrt{1+\beta^2}} - \frac{1}{2}\frac{\beta}{(1+\beta^2)^{3/2}}\right] \quad (29)$$

where β is now given by

$$\beta = \frac{a_k\rho_{1c}}{\sqrt{1-|\rho_1|^2}}. \quad (30)$$

Equation (29) is identical with the result of postdetection MRC [11], [12]. For nondiversity reception (we assume that branch 1 is always used), $w_1 = 1$ and $w_2 = 0$, and hence m and σ^2 in (23) are now given by $m = \rho_1(\sigma_1/\sigma_1')R_1^2$ and $\sigma^2 = \sigma_1^2(1-|\rho_1|^2)R_1^2$, where $R_1 = |z_1(k-1)|$. We can show that the conditional BER becomes $p_e(R_1) = 1/2\ \mathrm{erfc}\left[\{a_k\rho_{1c}/\sqrt{1-|\rho_1|^2}\}R_1/\sqrt{2\sigma_1'^2}\right]$. R_1 is Rayleigh distributed; its pdf is $p(R_1) = (R_1/\sigma_1'^2)\exp[-R_1^2/(2\sigma_1'^2)]$. The average BER can be derived easily using (B.4). The result is

$$P_e = \frac{1}{2}\left[1 - \frac{a_k\rho_{1c}}{\sqrt{1-\rho_{1s}^2}}\right]. \quad (31)$$

For frequency-selective fading, the differential detector input sample $z_l(k)$ is the sum of contributions from many multipaths with different time delays. Because the channel impulse response $g_l(\tau,t)$ is a complex Gaussian, $z_l(k)$ also become a complex Gaussian variable for the given transmitted symbol sequence. Therefore, (27)–(31) can also be applied to evaluate the average BER due to delay spread by appropriately modifying σ_l, σ_l', and ρ_l, since $z_l(k)$ is affected by the ISI from adjacent symbols (this will be discussed in Section IV-C).

B. Multiplicative Fading Case

To calculate BER using (27)–(31), we need w_2/w_1, σ_2/σ_1, σ_2'/σ_1', ρ_1, and ρ_2. In urban areas, the multipath channel is generated from the many obstacles, such as buildings, that surround the mobile station. A commonly accepted statistical model to describe this channel is that the multipath waves arrive at the mobile station antennas from all directions uniformly with equal amplitude [8]. In this case, the antenna gain difference affects equally the statistical properties of the desired signal and CCI. Consequently, all branches have the same average SIR, i.e., $\Lambda_l = \Lambda$. Furthermore, the fading correlation becomes $\eta = J_0(2\pi f_D T)$ [8], where f_D is the so-called maximum Doppler frequency given by mobile station traveling speed/carrier wavelength ($f_D = 46$ Hz at a travelling speed of 50 km/h and 1 GHz carrier frequency) and $J_0(\cdot)$ is the zeroth-order first kind Bessel function. We denote the average E_s/N_0 of the first branch by Γ instead of Γ_1 and assume that the average E_s/N_0 of the second branch is $q(\leqq 1)$ times smaller. To summarize, the parameters used in Section III are now given as follows: $q_{sl} = q_{il} = 1$, $q_{s2} = q_{i2} = q$, $\Gamma_1 = \Gamma$, $\Gamma_2 = q\Gamma$, $\Lambda_1 = \Lambda_2 = \Lambda$ and $\eta = J_0(2\pi f_D T)$. In this situation, the weight ratio w_2/w_1 is

$$\frac{w_2}{w_1} = q\frac{\Gamma+\Lambda}{q\Gamma+\Lambda}\frac{2\Gamma\Lambda+\Gamma+\Lambda}{q(2\Gamma\Lambda+\Gamma)+\Lambda}$$

(optimized for AWGN + CCI, see (18))

q^{-1}(optimized only for random FM noise, see (21)). (32)

Other parameters are, from (13), given by

$$\frac{\sigma_2}{\sigma_1} = \sqrt{\frac{q(1+\Lambda^{-1})+\Gamma^{-1}}{1+\Gamma^{-1}+\Lambda^{-1}}}, \qquad \frac{\sigma_2'}{\sigma_1'} = \frac{\sigma_2}{\sigma_1}$$

$$\rho_1 = \frac{J_0(2\pi f_D T)}{1+\Gamma^{-1}+\Lambda^{-1}}\exp j\Delta\phi(k),$$

$$\rho_2 = \frac{qJ_0(2\pi f_D T)}{q(1+\Lambda^{-1})+\Gamma^{-1}}\exp j\Delta\phi(k). \quad (33)$$

$$\alpha = \frac{2\frac{\sigma_2'^2}{\sigma_1'^2}\sin(2\psi)}{\left[\left(\frac{\sigma_2'^2}{\sigma_1'^2}-1\right)\cos(2\psi)+\frac{\sigma_2'^2}{\sigma_1'^2}+1\right]^2}$$

$$\beta = a_k \frac{\left(\rho_{1c}\frac{\sigma_2'}{\sigma_1'} - \rho_{2c}\frac{w_2}{w_1}\frac{\sigma_2}{\sigma_1}\right)\cos(2\psi) + \rho_{1c}\frac{\sigma_2'}{\sigma_1'} + \rho_{2c}\frac{w_2}{w_1}\frac{\sigma_2}{\sigma_1}}{\sqrt{\left[1-|\rho_1|^2-\left(1-|\rho_2|^2\right)\frac{\sigma_2'^2}{\sigma_1'^2}\frac{w_2^2}{w_1^2}\right]\cos(2\psi)+\left[1-|\rho_1|^2+\left(1-|\rho_2|^2\right)\frac{\sigma_2'^2}{\sigma_1'^2}\frac{w_2^2}{w_1^2}\right]}\sqrt{\left(\frac{\sigma_2'^2}{\sigma_1'^2}-1\right)\cos(2\psi)+\frac{\sigma_2'^2}{\sigma_1'^2}+1}}. \quad (28)$$

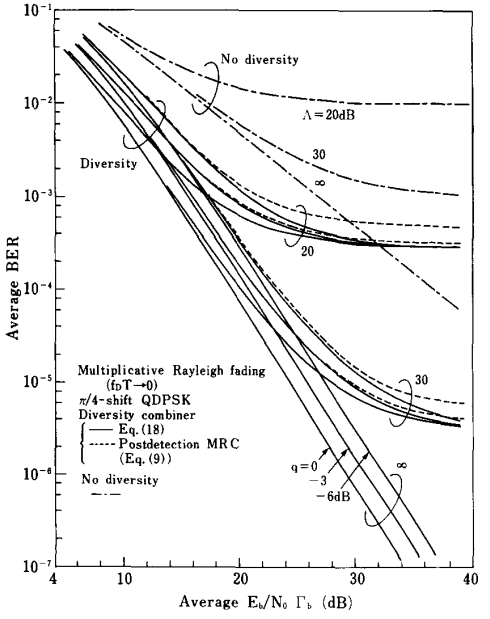

Fig. 3. BER performance with the combiner given by (18) as a function of average E_b/N_0 of the first branch for very slow multiplicative Rayleigh fading ($f_DT \to 0$) for power ratios $q = 0$, -3, and -6 dB. Average SIR= 20, 30, and ∞ dB.

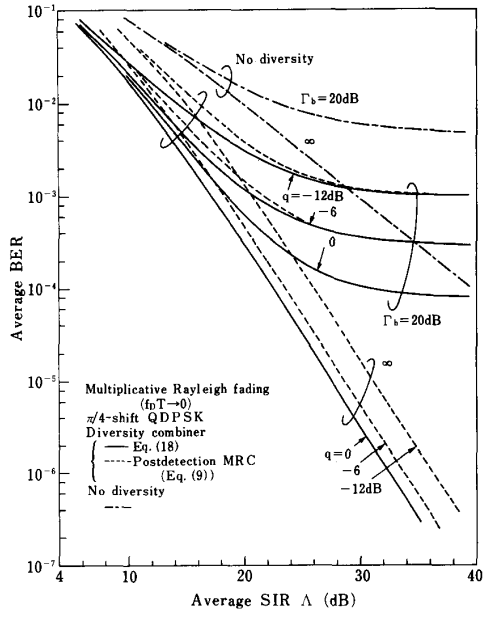

Fig. 4. BER performance with the combiner given by (18) as a function of average SIR for very slow multiplicative Rayleigh fading ($f_DT \to 0$) for power ratios $q = 0$, -6, and -12 dB. Average $E_b/N_0 = 20$ and ∞ dB.

The calculated BER performance for very slow Rayleigh fading ($f_DT \to 0$) is shown in Fig. 3 as a function of the average signal energy per bit-to-noise power spectrum density ratio $(E_b/N_0)\,\Gamma_b(=\Gamma/2)$ for power ratios $q = 0$, -3, and -6 dB. For the AWGN limited case ($\Lambda \to \infty$), the performance degrades as q decreases; the degradation in the value of Γ_b required to achieve a certain average BER is about 5 log q dB. On the other hand, when errors are predominantly caused by CCI ($\Gamma_b \to \infty$), the BER performance tends to be insensitive to q. This can be more clearly seen in Fig. 4, which shows the BER performance as a function of average SIR. For the CCI limited case ($\Gamma_b \to \infty$), the effect of unequal power between two branches can be completely mitigated. For comparison, the BER performance with postdetection MRC was calculated and plotted in Figs. 3 and 4. It can be seen from these figures that only for the AWGN limited case ($\Lambda \to \infty$), postdetection MRC provides BER performance almost identical to the optimal combiner. It can be easily understood from (18) or (32) that the optimal branch weight becomes the same for all branches at large Γ_b values when $\Lambda \to \infty$. However, when the CCI effect cannot be neglected, the BER performance with the postdetection MRC degrades as q decreases; Fig. 4 indicates that the degradation in the required value of Λ when $\Gamma_b \to \infty$ is about 1.2 and 3.8 dB for $q = -6$ and -12 dB, respectively.

Fig. 5 shows the BER performance optimized for random FM noise as a function of the normalized maximum Doppler frequency f_DT at average $E_b/N_0 = 20$ and ∞ dB. As in the CCI limited case, the performance is insensitive to q for very large average E_b/N_0 values. It should be noted that when AWGN is the major cause of errors, for example, $\Gamma_b = 20$ dB,

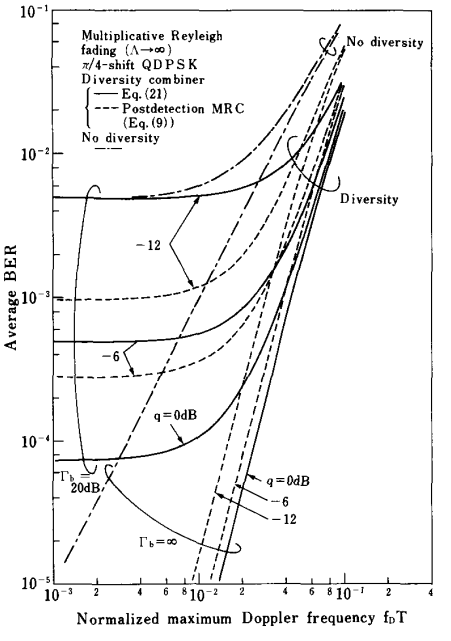

Fig. 5. BER performance with the combiner given by (21) as a function of the normalized maximum Doppler frequency f_DT for power ratios $q = 0$, -6, and -12 dB. Average $E_b/N_0 = 20$ and ∞ dB.

the BER performance with the weight given by (21) is inferior to that of postdetection MRC.

C. Frequency-Selective Fading

The analysis in Section III assumed multiplicative fading only. Here, we will find the optimal combiner in very slow

frequency-selective fading by evaluating the average BER using (27)–(31). The combiner output (5) can be rewritten as $v = v_1 + wv_2$, where $w = w_2/w_1$. Our problem is to find the optimum value of w. The BER calculation requires σ_2/σ_1, σ_2'/σ_1', ρ_1, and ρ_2, all of which will be derived in the following.

Frequency-selective fading is characterized by the delay power profile $\xi_l(\tau)$ defined as

$$\xi_l(\tau) = \left\langle |g_l(\tau,t)|^2 \right\rangle_{\text{time}}$$
$$\int_{-\infty}^{\infty} \xi_l(\tau)\, d\tau = 1\,. \tag{34}$$

The rms delay spread is an important parameter which governs the BER performance [7]–[13]. It is defined as

$$\tau_{\text{rms}} = \sqrt{\int_{-\infty}^{+\infty} \tau^2 \xi_l(\tau)\, d\tau - \left[\int_{-\infty}^{+\infty} \tau \xi_l(\tau)\, d\tau\right]^2}\,. \tag{35}$$

Assuming that $g_l(\tau,t)$ at any time delay τ is the sum of many independent impulses arriving from all directions uniformly with equal amplitude, each impulse equally contributes to form both $g_1(\tau,t)$ and $g_2(\tau,t)$. The result is that the delay power profiles, $\xi_1(\tau)$ and $\xi_2(\tau)$, of both branches are identical and are hereafter denoted by $\xi(\tau)$. Therefore, even if the average power of each branch is different, the effect of delay spread on each branch can be assumed to be the same, as is true in the case of CCI limited channels (see Section IV-B).

To calculate BER, no CCI ($\Lambda \to \infty$) and very slow fading ($f_D T \to 0$) are assumed. The average received signal power of the second branch is assumed to be smaller than that of the first branch by a factor of q. Because of the ISI effect, σ_2/σ_1, σ_2'/σ_1', ρ_1, and ρ_2 are different from those for the multiplicative fading case. Recall that σ_l^2 is the average power of the lth branch detector input at $t = kT$ and $\sigma_l'^2$ is that taken at $t = (k-1)T$. From (2), we have (36) (for derivation, see Appendix C), where $d_s(t)$ is given by (3).

Several delay power profile shapes have been reported. If the normalized rms delay spread $\tau_{\text{rms}}/T > 0.1 \sim 0.2$, the profile shape affects the BER significantly; however, the improvement achieved by diversity reception diminishes rapidly. We are interested in the small rms delay spread region (i.e., $\tau_{\text{rms}}/T < 0.2$) within which our diversity reception can perform satisfactorily. In this region, the profile shape does not have profound impact [11], [12]. Hence, for simplicity of calculation, we assume the double spike delay power profile (many impulses with different time delays are grouped into two), i.e., $\xi(\tau) = 0.5\delta(\tau + \tau_{\text{rms}}) + 0.5\delta(\tau - \tau_{\text{rms}})$. In the calculations, a five-symbol sequence (detected symbol is the middle one) is used in order to take into account the ISI effect. For each five-symbol sequence, we obtain $d_s(kT)$ and $d_s((k-1)T)$ from (3) (roll-off factor $\alpha = 0.5$ is assumed here) and σ_2/σ_1, σ_2'/σ_1', ρ_1, and ρ_2 from (36), then the average BER for that sequence pattern is evaluated from (27) and (28). Average BER's are finally averaged over all sequence patterns.

Both the random FM noise and ISI due to delay spread are produced by the multipath fading itself. The optimal combiner under frequency-selective fading may be the same as that for random FM noise; therefore, it is anticipated that the weight given by (21) can be used. To find the optimal weight, the average BER's due to delay spread only ($f_D T \to 0$ and $\Gamma_b \to \infty$) at the normalized rms delay spread $\tau_{\text{rms}}/T = 0.005$ were calculated and are plotted in Fig. 6 as a function of the weight ratio w for power ratios $q = 0$, -6, and -12 dB. It can be seen from this figure that the BER is minimized when $w = q^{-1}$ as was anticipated. The calculated average BER performance with $w = q^{-1}$ is shown in Fig. 7 as a function of τ_{rms}/T. The BER performance can be significantly improved, and furthermore, the performance is insensitive to q (i.e., the effect of unequal power is completely mitigated) when the delay spread is the single cause of errors. For comparison, the result for postdetection MRC is also plotted. When most errors are caused by AWGN (for very small values of τ_{rms}/T), postdetection MRC is superior. This is because the weight used is optimal only for the effect of delay spread (and also random FM noise). Therefore, it is necessary to identify the cause of errors to choose the appropriate weight, (18) or (21).

V. Comparison with Predetection MRC

Predetection MRC is assumed to predict perfectly the desired signal envelope and phase. The sum of AWGN and Rayleigh-faded CCI can be considered as Gaussian noise (see

$$\frac{\sigma_2}{\sigma_1} = \sqrt{\frac{q\int_{-\infty}^{+\infty}\xi(\tau)|d_s(kT-\tau)|^2\,d\tau + \Gamma^{-1}}{\int_{-\infty}^{+\infty}\xi(\tau)|d_s(kT-\tau)|^2\,d\tau + \Gamma^{-1}}},$$
$$\frac{\sigma_2'}{\sigma_1'} = \sqrt{\frac{q\int_{-\infty}^{+\infty}\xi(\tau)|d_s((k-1)T-\tau)|^2\,d\tau + \Gamma^{-1}}{\int_{-\infty}^{+\infty}\xi(\tau)|d_s((k-1)T-\tau)|^2\,d\tau + \Gamma^{-1}}}$$
$$\rho_1 = \frac{\int_{-\infty}^{+\infty}\xi(\tau)d_s(kT-\tau)\,d_s^*((k-1)T-\tau)\,d\tau}{\sqrt{\int_{-\infty}^{+\infty}\xi(\tau)|d_s(kT-\tau)|^2\,d\tau + \Gamma^{-1}}\sqrt{\int_{-\infty}^{+\infty}\xi(\tau)|d_s((k-1)T-\tau)|^2\,d\tau + \Gamma^{-1}}}$$
$$\rho_2 = \frac{q\int_{-\infty}^{+\infty}\xi(\tau)d_s(kT-\tau)\,d_s^*((k-1)T-\tau)\,d\tau}{\sqrt{q\int_{-\infty}^{+\infty}\xi(\tau)|d_s(kT-\tau)|^2\,d\tau + \Gamma^{-1}}\sqrt{q\int_{-\infty}^{+\infty}\xi(\tau)|d_s((k-1)T-\tau)|^2\,d\tau + \Gamma^{-1}}} \tag{36}$$

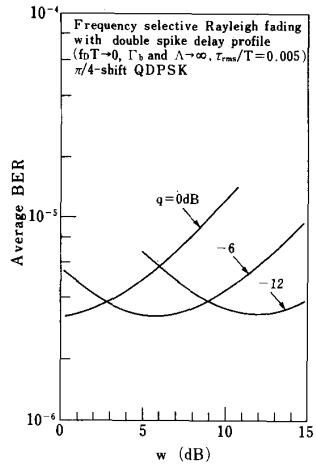

Fig. 6. Effect of weight ratio $w = w_2/w_1$ under very slow frequency selective Rayleigh fading ($f_DT \to 0$). Power ratio $q = 0$, -6, and -12 dB.

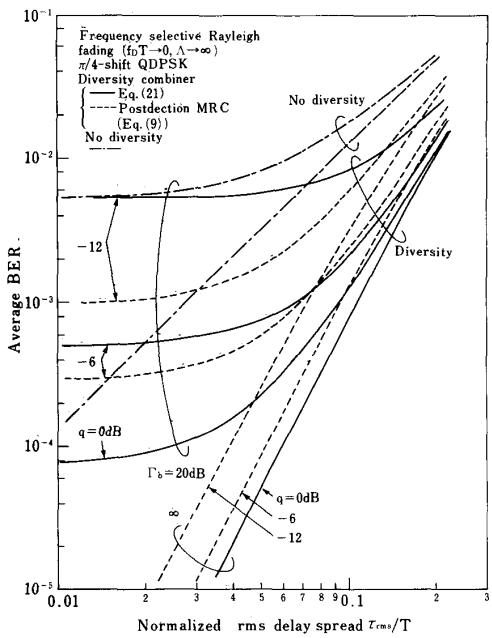

Fig. 7. BER performance with the combiner given by (21) as a function of the normalized rms delay spread $\tau_{\rm rms}/T$ for very slow frequency selective Rayleigh fading ($f_DT \to 0$) for power ratios $q = 0$, -6, and -12 dB. Average $E_b/N_0 = 20$ and ∞ dB.

Section III). Predetection MRC produces the output $z(k) = \sum_{l=1}^{L} w_{\mathrm{MRC}l} \cdot z_l(k)$. The lth branch weight $w_{\mathrm{MRC}l}$, which is now a complex value, is chosen so that the signal power-to-average noise (AWGN-plus-CCI) power ratio at the combiner output can be maximized. From (2), the instantaneous desired signal fading complex envelope is $u_l(k) = \sqrt{2E_{sl}/T}\, g_l(k)$ and the noise power is $N_l = E_{il}/T + N_0/T$. Thus, $w_{\mathrm{MRC}l}$ can be found from [7, ch. 10.5] as

$$w_{\mathrm{MRC}l} = \frac{u_l^*(k)}{N_l}. \tag{37}$$

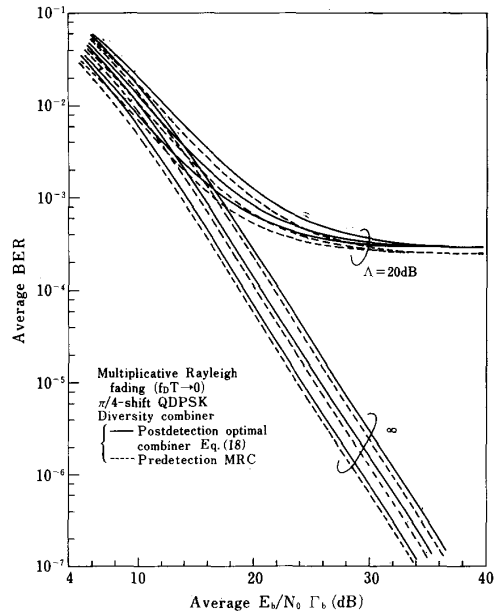

Fig. 8. Comparisoh of predetection MRC and postdetection optimal combiner.

On the other hand, for the postdetection optimal combiner, the weighted output of the lth branch differential detector is $v_l = w_l \cdot [z_l(k)z_l^*(k-1)]$; we rewrite this as $v_l = z_l(k)[w_l \cdot z_l(k-1)]^*$. Therefore, $w_l \cdot z_l(k-1)$ can be considered as the weighted reference. w_l is found from (18) to be given approximately by $w_l = 0.5a\Lambda_l/(\Gamma_l + \Lambda_l)$ for large values of Γ_l and Λ_l and $\eta = 1$ (very slow fading); letting $a = 2T/N_0$, we can show that $w_l = N_l^{-1}$. The weighted reference can be represented as

$$\text{weighted reference} = \frac{u_l(k-1)}{N_l} \exp j\phi(k-1) + \text{noise with unity variance} \tag{38}$$

which involves the modulation phase because differential detection is assumed. For very slow fading, $g_l(k) \sim g_l(k-1)$ and hence $u_l(k) \sim u_l(k-1)$; the weighting operation analogous to predetection MRC is implicit by differential detection and postdetection combining.

We compare the BER performance of $\pi/4$-shift QDPSK with two-branch predetection MRC and with postdetection optimal combiner under very slow multiplicative Rayleigh fading. The average BER calculation is described in Appendix D. Assuming the same conditions as in Section IV-B, the calculated results are shown in Fig. 8. For the AWGN limited case ($\Lambda \to \infty$), the performance difference is only about 0.4 dB irrespective of the values of the power ratio q. (The same result was also obtained for the CCI limited case ($\Gamma_b \to \infty$).) This slight degradation of postdetection diversity is attributed to the fact that the weighted reference in (38) is perturbed by noise.

VI. Conclusion

This paper analyzed the postdetection optimal diversity combiner for DPSK differential detection in the presence of Rayleigh fading and CCI. The postdetection MRC that combines all the detector outputs with equal weight is optimal only when the average power on each branch is the same. When CCI (random FM noise) is the single cause of errors, the branch weight should be inversely proportional to the average CCI (desired signal) power. The average BER performance of differentially detected $\pi/4$-shift QDPSK was numerically evaluated for the practical two-branch diversity case. It was shown that with optimal diversity, the effect of two branches with unequal power can be completely mitigated when either CCI or random FM noise is the single cause of error. Numerical BER calculations showed that the optimal combiner for frequency-selective Rayleigh fading is the same as that optimized for random FM noise. In addition, it was shown that the weighting operation analogous to predetection MRC is implicit with differential detection and postdetection combining; the BER performance is only about 0.4 dB degraded from that of predetection MRC.

Appendix A

$z_l(k-1)$ is a complex Gaussian variable with mean $s_r(k-1) = \sqrt{2E_{sl}/T}\exp j[\phi(k-1)+\theta_l]$ and variance N_0/T. Its pdf is given by

$$p(z_l(k-1)|s_r(k-1)) = \frac{1}{2\pi N_0/T} \cdot \exp\left[-\frac{|z_l(k-1)-s_r(k-1)|^2}{2N_0/T}\right]. \tag{A.1}$$

Consider the log-likelihood function for $s_r(k-1)$, which is expressed as (A.2), shown at the bottom of the page. The best estimate of $s_r(k-1)$ in the sense that the log-likelihood is maximized can be found from

$$\frac{\partial \log p(z_l(k-1)|s_r(k-1))}{\partial \operatorname{Re}[s_r(k-1)]} = -\frac{\operatorname{Re}[s_r(k-1)] - \operatorname{Re}[z_l(k-1)]}{N_0/T} = 0$$
$$\frac{\partial \log p(z_l(k-1)|s_r(k-1))}{\partial \operatorname{Im}[s_r(k-1)]} = -\frac{\operatorname{Im}[s_r(k-1)] - \operatorname{Im}[z_l(k-1)]}{N_0/T} = 0. \tag{A.3}$$

Equation (A.3) implies that the best estimate of $s_r(k-1)$ is $z_l(k-1)$. This can be intuitively understood from the fact that $z_l(k-1)$ is distributed symmetrically over two-dimensional space and the pdf of $z_l(k-1)$ peaks at $z_l(k-1) = s_r(k-1)$. Therefore, it is reasonable to infer that $s_r(k-1)$ is $z_l(k-1)$. Similar analysis can be found in [15].

Appendix B

Average BER calculation can be expressed as

$$Pe = \int_0^\infty dR \int_0^{\frac{\pi}{2}} d\psi \frac{1}{2} \operatorname{erfc}\left[a\frac{R}{\sqrt{2}}\right] cR^3 \exp\left[-b\frac{R^2}{2}\right] \tag{B.1}$$

where

$$a = \frac{w_1(a_k\rho_{1c})(\sigma_1/\sigma_1')\cos^2\psi + w_2(a_k\rho_{2c})(\sigma_2/\sigma_2')\sin^2\psi}{\sqrt{w_1^2\sigma_1^2\left(1-|\rho_1|^2\right)\cos^2\psi + w_2^2\sigma_2^2\left(1-|\rho_2|^2\right)\sin^2\psi}}$$
$$b = \frac{\cos^2\psi}{\sigma_1'^2} + \frac{\sin^2\psi}{\sigma_2'^2}, \qquad c = \frac{\sin\psi\cos\psi}{\sigma_1'^2\sigma_2'^2}. \tag{B.2}$$

Using $d\left(\exp[-bR^2/2]\right)/dR = -bR\exp[-bR^2/2]$, integration with respect to R of (B.1) is

$$I = \frac{c}{b}\int_0^\infty \operatorname{erfc}\left[a\frac{R}{\sqrt{2}}\right] R\exp\left[-b\frac{R^2}{2}\right] dR - \frac{a}{b\sqrt{2\pi}}\int_0^\infty R^2\exp\left[-\left(a^2+b\right)\frac{R^2}{2}\right] dR. \tag{B.3}$$

Using

$$\int_0^\infty x^2\exp\left[-ax^2\right] dx = \frac{1}{4}\sqrt{\frac{\pi}{a^3}}$$
$$\int_0^\infty x\exp\left[-a^2x^2\right]\operatorname{erfc}[bx]\,dx = \frac{1}{2a^2}\left[1-\frac{b}{\sqrt{a^2+b^2}}\right]. \tag{B.4}$$

Equation (B.3) becomes

$$I = \frac{c}{b^2}\left[1 - \frac{a/\sqrt{b}}{\sqrt{a^2/b+1}} - \frac{1}{2}\frac{a/\sqrt{b}}{(a^2/b+1)^{3/2}}\right]. \tag{B.5}$$

Finally, letting $\alpha = c/b^2$ and $\beta = a/\sqrt{b}$, (27) is obtained.

Appendix C

We use (2). Since we are assuming very slow fading and that the multipath channel impulse response $g_l(\tau,t)$ is composed of many independent impulses,

$$\langle g_l(\tau,kT)g_l^*(\mu,(k-1)T)\rangle \approx \langle g_l(\tau,kT)g_l^*(\mu,kT)\rangle = \xi(\tau)\delta(\tau-\mu) \tag{C.1}$$

$$\log p(z_l(k-1)|s_r(k-1)) = -\log(2\pi N_0/T) - \frac{|z_l(k-1)|^2 - 2\operatorname{Re}\{z_l(k-1)\cdot s_r^*(k-1)\} + |s_r(k-1)|^2}{2N_0/T}. \tag{A.2}$$

where $\xi(\tau)$ is the already defined delay power profile. For a squareroot Nyquist receiver filter, the noise samples, $z_{nl}(k)$ and $z_{nl}(k-1)$, have the power of N_0/T and are independent, where N_0 is the single-sided AWGN power spectrum density. Using (C.1), we obtain

$$\begin{aligned}
\frac{1}{2}\left\langle |z_l(k)|^2 \right\rangle &= \frac{E_{sl}}{T}\int_{-\infty}^{+\infty} d\tau \int_{-\infty}^{+\infty} d\mu \\
&\quad \cdot d_s(kT-\tau)\, d_s^*(kT-\mu) \\
&\quad \cdot \langle g_l(\tau, kT) g_l^*(\mu, kT)\rangle \\
&\quad + \frac{1}{2}\left\langle |z_{nl}(k)|^2 \right\rangle \\
&= \frac{E_{sl}}{T}\int_{-\infty}^{+\infty} \xi(\tau) \\
&\quad \cdot \left| d_s(kT-\tau)^2 \right| d\tau + \frac{N_0}{T} \\
\frac{1}{2}\left\langle |z_l(k-1)|^2 \right\rangle &= \frac{E_{sl}}{T}\int_{-\infty}^{+\infty} d\tau \int_{-\infty}^{+\infty} d\mu \\
&\quad \cdot d_s((k-1)T-\tau) \\
&\quad \cdot d_s^*((k-1)T-\mu) \\
&\quad \cdot \Big\langle g_l(\tau,(k-1)T) \\
&\qquad \cdot g_l^*(\mu,(k-1)T)\Big\rangle \\
&\quad + \frac{1}{2}\left\langle |z_{nl}(k-1)|^2 \right\rangle \\
&= \frac{E_{sl}}{T}\int_{-\infty}^{+\infty} \xi(\tau) \\
&\quad \cdot |d_s((k-1)T-\tau)|^2 d\tau + \frac{N_0}{T} \\
\frac{1}{2}\langle z_l(k) z_l^*(k-1)\rangle &= \frac{E_{sl}}{T}\int_{-\infty}^{+\infty} d\tau \int_{-\infty}^{+\infty} d\mu \\
&\quad \cdot d_s^*(kT-\tau) \\
&\quad \cdot d_s^*((k-1)T-\mu) \\
&\quad \cdot \langle g_l(\tau, kT) g_l^*(\mu,(k-1)T)\rangle \\
&= \frac{E_{sl}}{T}\int_{-\infty}^{+\infty} \xi(\tau)\, d_s(kT-\tau) \\
&\quad \cdot d_s^*((k-1)T-\tau)\, d\tau . \qquad \text{(C.2)}
\end{aligned}$$

Finally, letting $E_{sl}/N_0 = \Gamma_l$, we obtain $\sigma_l^2 (= 1/2\langle |z_l(k)|^2\rangle)$, $\sigma_l'^2 (= 1/2\langle |\ z_l(k-1)\ |^2\rangle)$, and $\rho_l (= 1/2\langle z_l(k) z_l^*(k-1)\rangle /(\sigma_l \sigma_l'))$ which are given by (36).

Appendix D

The conditional BER for $\pi/4$-shift QDPSK for the given power ratio γ of desired signal and AWGN-plus-CCI is given by [13, eq. (25)]

$$p_e = \frac{1}{4\pi\sqrt{2}}\int_0^{2\pi} \frac{1}{1-\frac{\cos t}{\sqrt{2}}} \exp\left[-\gamma\left(1-\frac{\cos t}{\sqrt{2}}\right)\right] dt . \qquad \text{(D.1)}$$

For predetection MRC, γ is given by

$$\begin{aligned}
\gamma &= \frac{\frac{1}{2}\left|\sum_{l=1}^{L} w_{\mathrm{MRC}l}\cdot\sqrt{\frac{2E_{sl}}{T}}\, g_l(k)\right|^2}{\sum_{l=1}^{L} |w_{\mathrm{MRC}l}|^2 \cdot N_l} \\
&= \sum_{l=1}^{L} \frac{\Gamma_l}{\Gamma_l/\Lambda_l + 1}\, |g_l(k)|^2 . \qquad \text{(D.2)}
\end{aligned}$$

Recall that $g_l(k)$'s are the independent complex Gaussian variables with unity variance. The pdf of $|g_l(k)|^2$ is $p(|g_l(k)|^2) = \exp -|g_l(k)|^2$. Substituting (D.2) into (D.1) and averaging with respect to all $|g_l(k)|^2$'s leads to the following average BER with predetection MRC:

$$Pe = \frac{1}{4\pi\sqrt{2}}\int_0^{2\pi} \cdot \frac{dt}{\left(1-\frac{\cos t}{\sqrt{2}}\right)\prod_{l=1}^{L}\left[1+\frac{\Gamma_l}{\Gamma_l/\Lambda_l+1}\left(1-\frac{\cos t}{\sqrt{2}}\right)\right]} . \qquad \text{(D.3)}$$

The above integration can be numerically performed.

References

[1] F. G. Jenks, P. D. Morgan, and C. S. Warren, "Use of four-level phase modulation for digital mobile radio," *IEEE Trans. Electromagn. Compat.*, vol. EMC-14, pp. 113–128, Nov. 1972.

[2] Y. Akaiwa, and Y. Nagata, "Highly efficient digital mobile communications with a linear modulation method," *IEEE J. Select. Areas Commun.*, vol. SAC-5, pp. 890–895, June 1987.

[3] J. A. Tarallo and G. I. Zysman, "Modulation techniques for digital cellular systems," in *Proc. 38th IEEE VTC,* Philadelphia, PA, June 15–17, 1988, pp. 245–248.

[4] K. Ohno and F. Adachi, "Effects of post detection selection diversity reception in QDPSK land mobile radio," *Electron. Lett.*, vol. 25, pp. 1293–1294, Sept. 1989.

[5] J. Uddenfeldth, K. Raith, and B. Hedberg, "Digital technologies in cellular radio," in *Proc. 38th IEEE VTC,* Philadelphia, PA, June 15–17, 1989 pp. 516–519.

[6] N. Nakajima, M. Kuramoto, K. Kinoshita, and T. Utano, "A system design for TDMA mobile radio," in *Proc. 40th IEEE VTC,* FL, May 6–9, 1990, pp. 295–298.

[7] M. Schwartz, W. R. Bennett, and S. Stein, *Communication Systems and Techniques.* New York: McGraw-Hill, 1966.

[8] W. C. Jakes, Jr., ed., *Microwave Mobile Communications.* New York: Wiley, 1974.

[9] B. Glance and L. J. Greenstein, "Frequency-selective fading effects in digital mobile radio with diversity combining," *IEEE Trans. Commun.*, vol. COM-31, pp. 1085–1094, Sept. 1983.

[10] M. V. Clark, L. J. Greenstein, K. Kennedy, and M. Shafi, "MMSE diversity combining for wide-band digital cellular radio," *IEEE Trans. Commun.*, vol. 40, pp. 1128–1135, June 1992.

[11] F. Adachi and J. D. Parsons, "Error rate performance of digital FM mobile radio with postdetection diversity," *IEEE Trans. Commun.*, vol. 37, pp. 20–210, Mar. 1989.

[12] F. Adachi and K. Ohno, "BER performance of QDPSK with postdetection diversity reception in mobile radio channels," *IEEE Trans. Veh. Technol.*, vol. 40, pp. 237–249, Feb. 1991.

[13] F. Adachi, K. Ohno, and M. Ikura, "Postdetection selection diversity reception with correlated, unequal average power Rayleigh fading signals for $p/4$-shift QDPSK mobile radio," *IEEE Trans. Veh. Technol.*, vol. 41, pp. 199–210, May 1992.

[14] K. Tunekawa, "Diversity antennas for portable telephones," in *Proc. 39th IEEE VTC,* San Francisco, CA, May 1–3, 1989, pp. 50–56.

[15] H. B. Voelcker, "Phase-shift keying in fading channels," *Proc. Inst. Elect. Eng.*, vol. 107, pt. B, pp. 31–38, Jan. 1960.

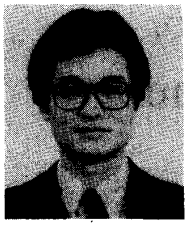

Fumiyuki Adachi (M'79–SM'90) graduated from Tohoku University, Japan in 1973 and received the Dr. Eng. from the same university in 1984.

In 1973 he joined the Nippon Telegraph & Telephone Corporation (NTT) Laboratories in Japan, where his major research activities centered on mobile communication signal processing, including digital modulation/demodulation, diversity reception, and channel coding. In July 1992, he transferred to NTT Mobile Communications Network, Inc., where he continues the same research activities. During the academic year of 1984/85, he was United Kingdom SERC Visiting Research Fellow at the Department of Electrical Engineering and Electronics of Liverpool University. He authored chapters for three books: Y. Okumura and M. Shinji, Eds., *Fundamentals of Mobile Communications* (in Japanese) IEICI, Japan, 1986; M. Shinji, Ed., *Mobile Communications* (in Japanese) Maruzen, 1989; and M. Kuwabara Ed., *Digital Mobile Communications* (in Japanese) Kagaku Simbun-sha, 1992. He was a member of IEEE Communications Society Asian Pacific Committee from 1986 to 1989. He was a treasurer in 1990, and has been a secretary of IEEE Vehicular Technology Society Tokyo Chapter since 1991.

Dr. Adachi is a co-recipient of the IEEE Vehicular Technology Society Paper of the Year Award in 1980 and 1990. He is a member of the Institute of Electronics, Information, and Communication Engineers of Japan.